Design and kinematics Analysis of Folding Mechanism of Patient Stretcher

Shaoxin Wen [1,2], Xinzui Wang [1,3,*], Fucheng Cao[1], Hui Fu[2]

[1]Ji Hua Laboratory, Foshan 528200, China;
[2]School of Mechanical and Electrical Engineering, Guangdong University of Technology, Guangzhou 510006, China;
[3]Suzhou Institute of Biomedical Engineering and Technology, Chinese Academy of Sciences, Suzhou 215163, China

*Corresponding author:wangxz@jihualab.com

ABSTRACT. The transfer and transportation of patients have always been important issues in home care and hospital care. With the acceleration of the world's aging population, the number of disabled and semi disabled elderly people is constantly expanding, and this problem is becoming increasingly prominent. In order to address this issue, this article has preliminarily designed a foldable wheelchair stretcher that can meet the actual needs of patients after transportation. The main work of this study is as follows: (1) Design the back lifting and leg bending mechanisms of wheelchair stretchers; (2) Analyze the back lifting and leg bending mechanisms and select driving components; (3) Kinematics analysis is carried out for the two driving modes of the back lifting mechanism to select a more appropriate one.

Keywords: Patient Stretcher, foldable, Structure Design, kinematics Analysis

1   Introduction

According to United Nations data, by 2019, the global population of elderly people aged 65 and above reached 703 million, and it is expected to double again by 2050 [1]. With the continuous deepening of global aging, the number of disabled and semi disabled individuals due to age and disease is increasing. For every elderly person with limited mobility, they yearn to be able to travel in a wheelchair and bask in more sunlight outdoors, but these simple daily activities are difficult for them to achieve [2]. In order to solve this problem, a large number of convenient transportation tools for patients have been developed [3, 4]. In 1997, the Massachusetts Institute of Technology developed a nursing bed called RHOMBUS [5], which can display bed chair separation through remote control. Panasonic, a Japanese company, has developed a "machine bed and chair" called Resyone, which can achieve deformation between beds and wheelchairs, becoming the world's first professionally certified medical robot product [6]. Beijing University of Aeronautics and Astronautics in China has developed a multifunctional bed chair integrated nursing bed, suitable for disabled elderly people with

normal intelligence [7]. The above studies all used bed and chair separation to transfer patients for transportation, but this method requires very high docking technology. The transfer equipment for transferring patients from hospital beds to stretchers is relatively mature, such as the bed transfer robot developed by Wang Hobo's team at Yanshan University in China [8]; Maxi move, a bucket type transfer machine invented by ArjoHuntleigh Company in Sweden [9]. Therefore, in order to meet the travel needs of patients after bed transfer, it is necessary to study wheelchair stretchers. The core mechanism of the wheelchair stretcher is the back lifting and leg bending mechanism. Therefore, this paper mainly designs and analyzes the back lifting and leg bending mechanisms and selects their actuator. Finally, kinematics analysis is carried out on the back lifting mechanism to select an appropriate driving mode for it, so as to ensure the stability of the deformation process and patient comfort.

2   Design of the Deformation Folding Mechanism for Stretcher Carts

The purpose of designing a foldable mechanism is to enable the stretcher to switch between wheelchair mode and hospital bed mode, and its movements are mainly divided into back lifting and leg bending movements. The four major parts of a standard wheelchair stretcher car are the back plate, seat plate, leg plate, and foot plate. Based on the ergonomics theory and anthropometry principle, combined with the size standards of domestic sickbeds and wheelchairs, the size distribution of stretchers in the sickbed mode is shown in Figure 1.
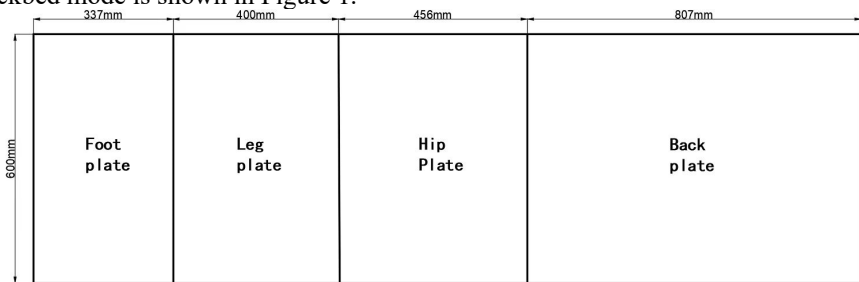

Fig. 1. Size distribution diagram

The installation space of the stretcher truck is limited, and the folding mechanism should be designed as simple and compact as possible while ensuring practicality. The structure of the folding part of the stretcher designed in this article in wheelchair mode is shown in Figure 2. The seat plate is connected to the chassis, and its position remains unchanged during the deformation process of the stretcher truck. Hinge connections are used between the back plate and the sitting plate, the sitting plate and the leg plate, and the leg plate and foot plate. The back actuator is installed below the back plate, and the rotation of the back plate is achieved by controlling the expansion and contraction of the linear actuator, with a rotation range of 0-85 °. The leg actuator is installed under

the sitting board, and the principle of leg bending motion is similar to back lifting motion, with a rotation range of 0-45 °.
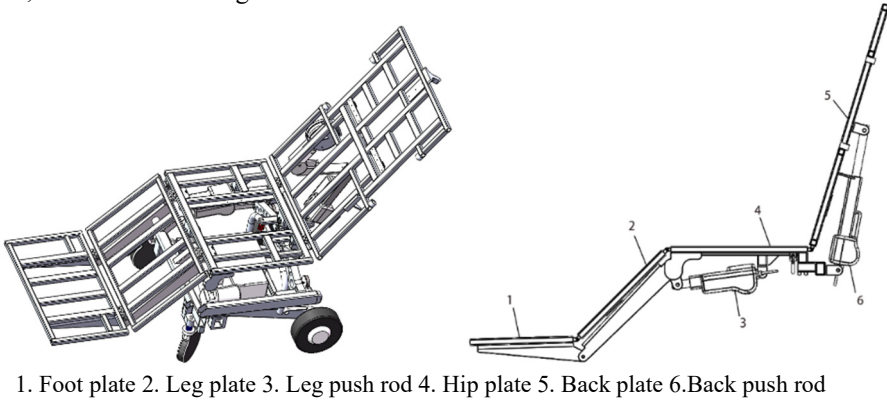

1. Foot plate 2. Leg plate 3. Leg push rod 4. Hip plate 5. Back plate 6.Back push rod

Fig. 2. Stretcher folding diagram

3   Selection of driving components

Linear actuator is a driving device that can convert rotary motion into linear motion. It has the advantages of compact structure, good self-locking performance, and fast response [10], making it very suitable for application in the field of medical equipment. Therefore, the power components of the lifting back and bending leg mechanism of the wheelchair bed use linear actuator. The back lifting motion of the wheelchair bed is achieved through the push and pull of a linear actuator, as shown in the diagram. When the back plate rotates around point O, the trajectory of the action point of the electric on the back plate is a circle with a radius of OD, and the rotation angle range of the back plate is 0-85 °. During the patient's transition from lying to sitting, the linear actuator continuously elongates, and vice versa.

The back lifting motion of the wheelchair bed is achieved through the push and pull of a linear actuator, as shown in Figure 3. When the back plate rotates around point O, the trajectory of the action point of the linear actuator on the back plate is a circle with a radius of OD, and the rotation angle range of the back plate is 0-85 °. During the patient's transition from lying to sitting, the linear actuator continuously elongates, and vice versa.

Fig. 3. Schematic diagram of back lifting structure

When the patient is lying flat and the lifting angle of the back plate is 0 °, the length FD' of the linear actuator is the shortest:

$$FD' = \sqrt{(OE - CD)^2 + (OC - EF)^2} \tag{1}$$

$$OF = \sqrt{OE^2 + EF^2} \tag{2}$$

When the patient is in a back lifting state, the lifting angle of the back plate is 85 °, and at this moment, the length FD of the linear actuator is the longest.

In the ΔCOD, there are:

$$OD = \sqrt{OC^2 + CD^2} \tag{3}$$

$$\angle COD = \arctan \frac{CD}{OC} \tag{4}$$

$$\angle FOD = \angle HOF + \alpha - \angle COD \tag{5}$$

In the ΔFOD, there are:

$$FD = \sqrt{OF^2 + OD^2 - 2OF \cdot OD \cos \angle FOD} \tag{6}$$

The stretching amount of the actuator during the back lifting movement is:

$$\Delta l = FD - FD' \tag{7}$$

In this article, it is assumed that the total weight of the human body is 100kg. Through actual measurement, it is found that the weight above the back of the human

body accounts for 63% of the total weight, which means m_1=63kg. The weight of the stretcher truck's back plate, m_2, is approximately 10kg.

$$F_1 = (m_1 + m_2)g\cos\alpha \tag{8}$$

So, taking point O as the rotation point, establish the torque balance equation as follows:

$$F_1 \cdot \frac{1}{2}OB = F_2 \cdot OD \cdot \sin\angle FOD \tag{9}$$

Which means that:

$$F_2 = \frac{F_1 \cdot OB}{2OD \cdot \sin\angle FOD} \tag{10}$$

Combine the equation of (1) - (10), where OC=408mm, EF=83.9mm, OE=65mm, CD=50mm, m_1=63kg, m_2=10kg.
Using MATLAB software, plot the change curve of the length FD of the linear actuator and the change curve of the thrust. From Figure 4, it can be seen that during the back lifting process, the initial length of the push rod is 324.5mm, the maximum length is 467.09mm, and the required stroke $\Delta l = 142.59$mm. From Figure 5, it can be seen that as the rotation angle increases, the thrust of the back plate linear actuator continues to decrease. When the rotation angle $\alpha = 0°$, the maximum thrust of the linear actuator is 2976.97N, and when the rotation angle $\alpha = 85°$, the minimum thrust of the linear actuator is 259.46N.
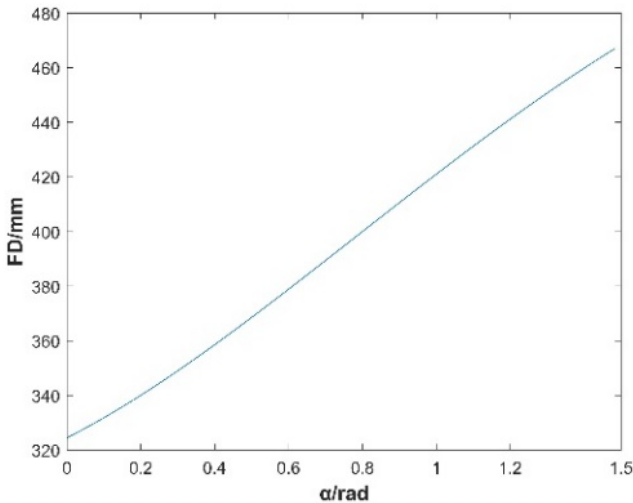
Fig. 4. Change in length of linear actuato
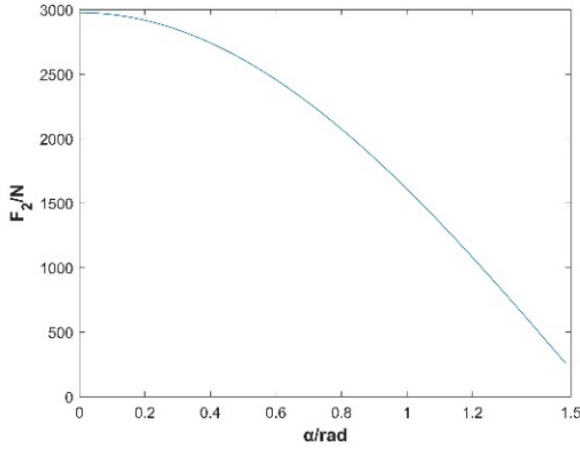
Fig. 5. Change in force of linear actuator

Similarly, the selection of the leg plate linear actuator was carried out. Due to the complexity of the leg bending mechanism, the simplified motion diagram is shown in Figure 6. When the leg board rotates around point O, the trajectory of the action point of the linear actuator on the leg board is a circle with a radius of OD, and the rotation angle range of the back board is 0-45 °. During the patient's transition from sitting to lying position, the linear actuator continuously shortens, and vice versa.
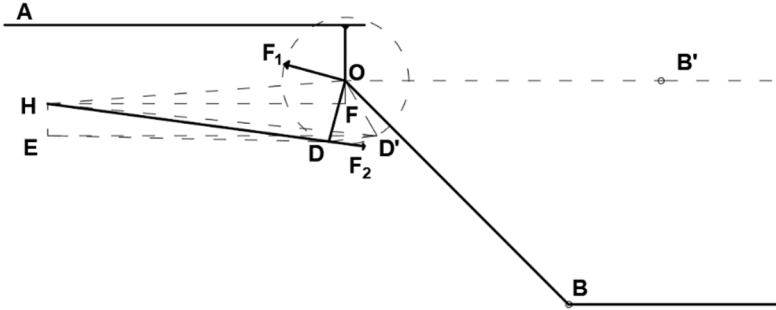
Fig. 6. Schematic diagram of leg bending structure

When the patient is lying flat, the bending angle of the leg board is 0 °, and the maximum length of the linear actuator at this moment is HD'.
In the ΔHED, there are:

$$HD' = \sqrt{HE^2 + ED'^2} \tag{11}$$

In the ΔHOD, there are:

$$OH = \sqrt{OF^2 + HF^2} \tag{12}$$

When the patient is in a sitting position, the bending angle of the leg board is 45 °, and the shortest length of the linear actuator is HD.

In the ΔODD', there are:

$$DD' = \sqrt{OD^2 + OD'^2 - 2OD \cdot OD' \cdot \cos\phi} \tag{13}$$

$$\angle OD'D = \frac{(\pi - \phi)}{2} \tag{14}$$

In the ΔED'D, there are:

$$\angle ED'D = \angle OD'D - \angle OD'E \tag{15}$$

$$ED = \sqrt{ED'^2 + ED^2 - 2ED' \cdot DD' \cdot \cos\angle ED'D} \tag{16}$$

$$\angle DED' = \arccos(\frac{ED'^2 + ED^2 - DD'^2}{2 \cdot ED' \cdot ED}) \tag{17}$$

In the ΔHED, there are:

$$\angle HED = \angle DED' + \frac{\pi}{2} \tag{18}$$

$$HD = \sqrt{EH^2 + ED^2 - 2EH \cdot ED \cdot \cos\angle HED} \tag{19}$$

The amount of extension and retraction of the push rod during leg bending movement is:

$$\varDelta l = HD' - HD \tag{20}$$

After the actual measurement results, it is known that the weight of the legs and feet of the human body accounts for approximately 30% of the total weight, that is, m_3 is 30kg, and the mass of the back board is approximately m_4 is 10kg. Therefore, there are:

$$F_2 = (m_3 + m_4)g \tag{21}$$

Using point O as the rotation point, establish the torque balance equation as:

$$F_2 = \frac{F_1 \cdot OD}{OD \cdot \sin\angle ODH} \tag{22}$$

The value of ∠ODH is:

$$\angle ODH = \arccos\frac{HD^2 + OD'^2 - OH^2}{2 \cdot HD \cdot OD'} \tag{23}$$

Combine the above formulas, where HE=30.1mm, ED'=312.6mm, HF=282.9mm, OF=22mm, OD=OD'=60mm, ∠ODH = 60 °. Using MATLAB software, plot the

change curve of the length HD of the linear actuator as shown in Figure 7 and the change curve of the thrust as shown in Figure 8. It can be seen that the initial length of the push rod is 314.7mm, and the minimum length is 269.5mm. And when the rotation angle α is 0 °, the maximum thrust of the linear actuator is 483.7N, and when the rotation angle α is 45 °, the thrust of the linear actuator is 392N.
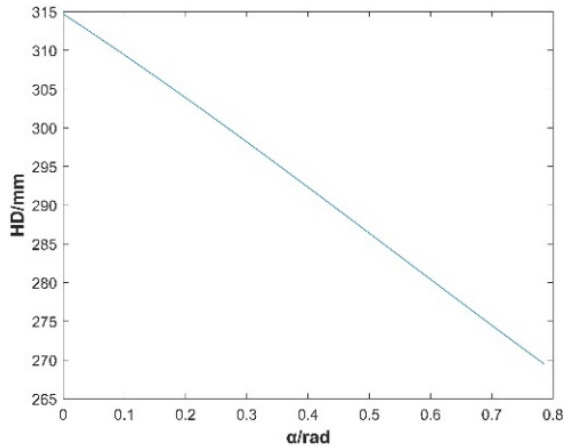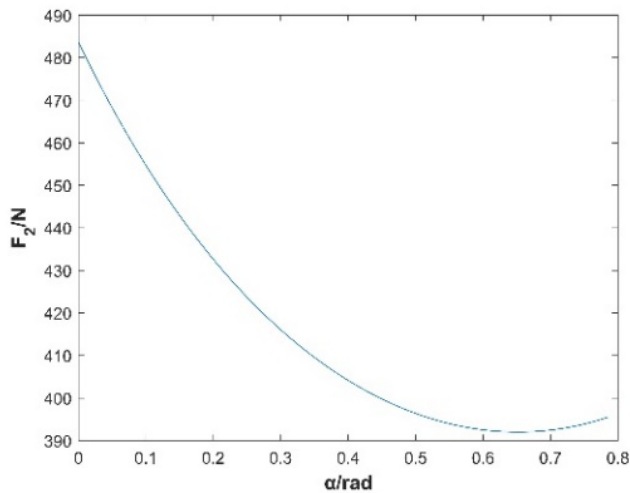

Fig. 7. Change in length of linear actuator

Fig. 8. Change in force of linear actuator

After the above analysis, the required parameters for the linear actuator for back lifting and leg bending movements have been established. For comprehensive consideration, the JC35W3 linear actuator model from Zhejiang JieChang Linear Drive Technology Co., Ltd. was ultimately selected, as shown in Figure 9.

Fig. 9. JC35W3 linear actuator

The characteristics of this linear actuator are high control accuracy, low noise, and good safety performance, which are suitable for medical devices and other fields. The key parameters of the linear actuator are shown in Table 1.

Table 1. JC35W3 linear actuator parameters

Rated voltage	Locking Force	Maximum Load	Maximum Speed	trip	Installation distance
24V	3000N	3000N	5.5mm/s	150mm	475mm

4   Motion Analysis and Simulation of Back Lifting Mechanism

In folding movements, the most affecting factor for patient comfort is the back lifting movement, so it is necessary to analyze the back lifting movement separately. The movement of the back lifting mechanism can be achieved through two driving methods. One is that the electric push rod moves at unequal speeds, driving the back plate to rotate at equal angular speeds; another method is for the electric push rod to move at a constant speed, while the back plate to move at an uneven speed. Therefore, this paper conducts motion calculation and simulation analysis for the two driving modes respectively, and tests whether they can meet the use requirements according to human comfort, bed structural stability and control stability, and selects one of the more appropriate driving modes. The schematic diagram of the back lifting mechanism of the deformable stretcher truck is shown in Figure 10.
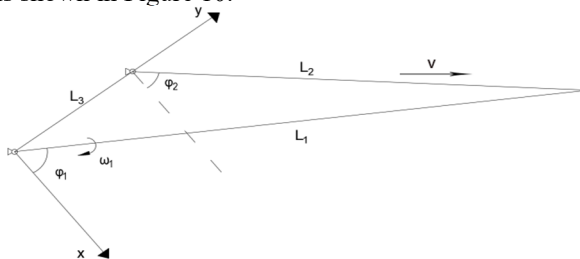

Fig. 10. Schematic diagram of back lifting mechanism

L_1 is the connecting line between the rotation point of the back plate and the support seat 2; L_2 is the length of the electric push rod; L_3 is the connecting line between the rotation point and the support seat 1; ω_1 is the angular velocity of the back rotation; v is the linear velocity of the electric push rod; Is the angle between φ_1 and the x-axis, and is the angle between φ_2 and the x-axis.

1. Perform location analysis:

The closed vector equation of this mechanism is:

$$L_1 = L_3 + L_2 \tag{24}$$

Namely:

$$L_1 e^{i\varphi_1} = L_3 + L_2 e^{i\varphi_2} \tag{25}$$

Applying Euler's Formula, $e^{i\gamma} = \cos\gamma + i\sin\gamma$ Separate the real and imaginary parts in the equation to obtain the following formula:

$$\begin{cases} L_1 \sin\varphi_1 = L_3 + L_2 \sin\varphi_2 \\ L_1 \cos\varphi_1 = L_2 \cos\varphi_2 \end{cases} \tag{26}$$

When the linear velocity v of the electric push rod is constant, there is:

$$\begin{cases} \varphi_1 = \arcsin \dfrac{L_1^2 + L_3^2 - L_2^2}{2L_1 L_3} \\ \varphi_2 = \arcsin \dfrac{L_1^2 - L_2^2 - L_3^2}{2L_2 L_3} \end{cases} \tag{27}$$

When the back plate rotates uniformly around the rotation point, ω_1 remains unchanged:

$$\tan\varphi_2 = \frac{L_1 \sin\varphi_1 - L_3}{L_1 \cos\varphi_1} \tag{28}$$

Calculate the length of the electric push rod based on the following formula after calculating ω_1 according to different situations:

$$L_2 = \frac{\cos\varphi_1}{\cos\varphi_2} \tag{29}$$

2. Perform speed analysis:

Taking the derivative of the equation (25) over time t yields the following:

$$iL_1\omega_1 e^{i\varphi_1} = iL_2\omega_2 e^{i\varphi_2} + ve^{i\varphi_2} \tag{30}$$

Multiplying $e^{-i\varphi_2}$ on both sides simultaneously yields:

$$iL_1\omega_1 e^{i(\varphi_1-\varphi_2)} = iL_2\omega_2 + v \tag{31}$$

By applying Euler's formula to expand, we can obtain:

$$iL_1\omega_1[\cos(\varphi_1-\varphi_2)+i\sin(\varphi_1-\varphi_2)] = iL_2\omega_2 + v \tag{32}$$

After separating the actual and imaginary parts, there are:

$$\begin{cases} L_1\omega_1\cos(\varphi_1-\varphi_2) = L_2\omega_2 \\ -L_1\omega_1\sin(\varphi_1-\varphi_2) = v \end{cases} \tag{33}$$

In the diagram, L1=411.05mm, L3=106.13mm, and the initial length of the electric push rod is 325mm. If the driving method is to choose a uniform motion of the electric push rod, based on comprehensive considerations such as human comfort, the speed is set to 5.28mm/s. By organizing the above formula, we can obtain:

$$\begin{cases} \omega_1 = \dfrac{-v}{L_1\sin(\varphi_1-\varphi_2)} \\ \omega_2 = \dfrac{-v\cot(\varphi_1-\varphi_2)}{L_2} \end{cases} \tag{34}$$

Use MATLAB software to draw the rotation angular velocity variation curve of L1, as shown in Figure 11. If the driving method is to choose a uniform rotation of the backplane, and the rotational angular velocity $\omega_1 = 0.055\text{rad/s}$, then:

$$\begin{cases} v = L_1\omega_1\sin(\varphi_1-\varphi_2) \\ \omega_2 = \dfrac{L_1\omega_1\cos(\varphi_1-\varphi_2)}{L_2} \end{cases} \tag{35}$$

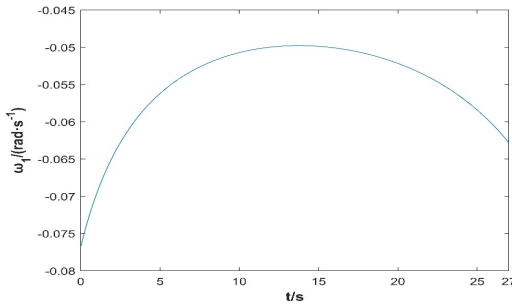Similarly, use MATLAB to draw the linear velocity variation curve of the electric push rod, as shown in Figure 12.

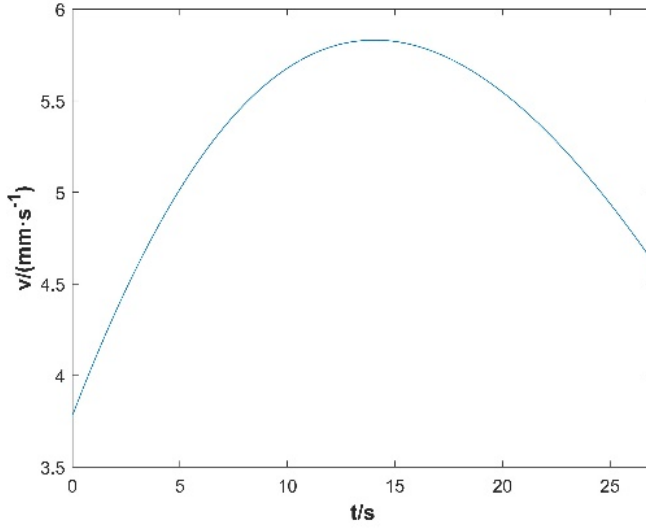**Fig. 11.** Changes in angular velocity of the back

Fig. 12. Change in velocity of linear actuator

3. Perform angular velocity analysis:

When the linear velocity v of the electric push rod remains constant, the derivative of the equation (30) with respect to time t is obtained as follows:

$$iL_1\alpha_1 e^{i\varphi_1} - L_1\omega_1^2 e^{i\varphi_1} = iv\omega_2 e^{i\varphi_2} + iL_2\alpha_2^2 e^{i\varphi_2} - L_2\omega_2^2 e^{i\varphi_2} + iv\omega_2 e^{i\varphi_2} \tag{36}$$

After Euler expansion, separating the real and imaginary parts yields:

$$\begin{cases} L_1\alpha_1 \sin(\varphi_1 - \varphi_2) + L_1\omega_1^2 \cos(\varphi_1 - \varphi_2) = L_2\omega_2^2 \\ L_1\alpha_1 \cos(\varphi_1 - \varphi_2) - L_1\omega_1^2 \cos(\varphi_1 - \varphi_2) = 2v\omega_2 + L_2\alpha_1 \end{cases} \tag{37}$$

That is to say, we obtain the following:

$$\begin{cases} \alpha_1 = \dfrac{L_2\omega_2^2}{L_1 \sin(\varphi_1 - \varphi_2)} - \dfrac{\omega_1^2 \cos(\varphi_1 - \varphi_2)}{\sin(\varphi_1 - \varphi_2)} \\ \alpha_2 = \dfrac{L_1\alpha_1 \cos(\varphi_1 - \varphi_2) - L_1\omega_1^2 \cos(\varphi_1 - \varphi_2) - 2v\omega_2}{L_2} \end{cases} \tag{38}$$

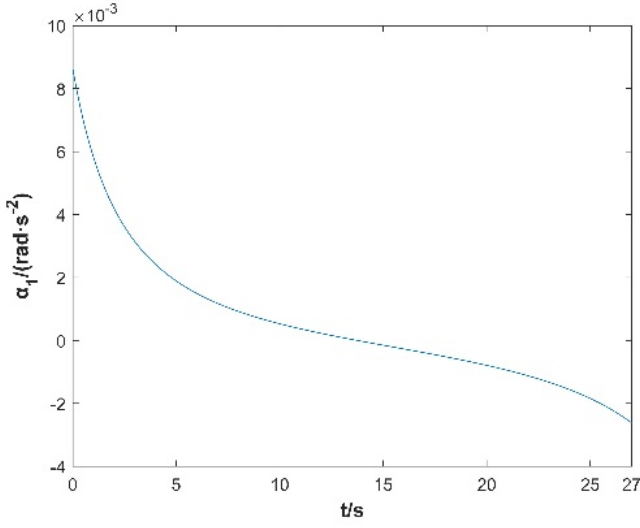Use MATLAB to draw the change curve of angular acceleration of its backplane rotation, as shown in Figure 13.
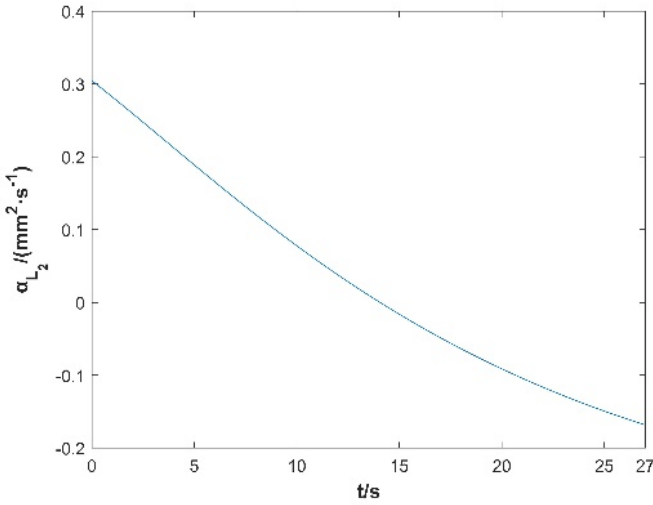
Fig. 13. Changes in angular acceleration of the back

Fig. 14. Change in acceleration of linear actuator

When the back plate rotates at angular velocity ω_1 when constant, taking the derivative of equation (30) over time t yields the following:

$$-L_1\omega_1^2 e^{i\varphi_1} = iv\omega e^{i\varphi_2} - L_2\omega_2^2 e^{i\varphi_2} + a_{L_2} e^{i\varphi_2} + iv\omega_2 e^{i\varphi_2} + iL_2\alpha_2 e^{i\varphi_2} \tag{39}$$

By expanding the Euler formula and separating the real and imaginary parts, it can be concluded that:

$$\begin{cases} L_1\omega_1^2 \sin(\varphi_1 - \varphi_2) = 2v\omega_2 + L_2\alpha_2 \\ a_{L_2} = L_2\omega_2^2 - L_1\omega_1^2 \cos(\varphi_1 - \varphi_2) \end{cases} \tag{40}$$

The variation curve of rod acceleration is shown in Figure 14.

Through the motion analysis of the two driving methods of the back lifting mechanism above, it can be seen that during the back lifting process, the speed and acceleration of both methods are relatively smooth and smooth, without any abnormal protrusions, and can meet the usage requirements. From the perspective of human kinematics, the patient will be more comfortable when the back plate rotates at a uniform speed, but it is difficult to control the non-uniform movement of the electric push rod at this time. And in this article, when the electric push rod is used for uniform motion in the back lifting structure, the changes in velocity and angular velocity are not significantly different from the previous method, and the control is simpler. Therefore, considering the driving method of the back lifting mechanism, the electric push rod is used for uniform motion.

5 Conclusions

This article proposes a simple and compact deformable stretcher folding mechanism based on the actual travel needs of disabled and semi disabled elderly people. Calculate the motion of the back lifting and leg bending mechanisms, and select the electric push rod based on this. In order to ensure the comfort of the patient during the deformation of the stretcher truck, two driving modes of the back lifting mechanism are discussed separately by means of kinematics analysis, and one of the appropriate driving modes is selected. The research content of this article lays the foundation for further research on the foldable stretcher vehicle, and also provides a way for other scholars who develop foldable stretcher vehicles to choose linear actuators and driving modes.

Acknowledgment

References

1. United Nations, Department of Economic and Social Affairs, Population Division. World Population Ageing 2019: Highlights (ST/ESA/SER.A/430). Accessed: May 6, 2020. https://www.un.org/en/development/desa/population/publications/pdf/ageing/WorldPopulationAgeing2019-Highlights.pdf.

2. JÄGER M, JORDAN C, THEILMEIER A, et al. (2013) Lumbar-load analysis of manual patient-handling activities for biomechanical overload prevention among healthcare workers [J]. Annals of Occupational Hygiene, 57(4): 528–544.   DOI: 10.1093/annhyg/mes088.

3. Simon W. H, "Storable Patient Lift and Transfer Apparatus" US: 5560054, 1996-10-1.

4. Evanoff B., Wolf L., Aton E., et al. (2003) Reduction in Injury Rates in Nursing Personnel through Introduction of Mechanical Lifts in the Workplace. American Journal of Industrial Medicine. pp.451-457, 2003. http://doi.org/ 10.1002/ajim.10294.

5. KUME Y, TSUKADA S, KAWAKAMI H. (2015) Design and evaluation of rise assisting bed "Resyone®" based on ISO 13482 [J]. Journal of the Robotics Society of Japan, 33(10): 781–788.

6. Hu M, Liu J, Chen D, et al. (2013) Integrated bed chair multifunctional nursing bed - realizing the dream of elderly bedridden people taking care of themselves [J]. Robot Technology and Applications. DOI: 10.3969/j.issn.1004-6437.2013.02.022.

7. Chen D, Fan Q, Zhao C, et al. (2011) A multifunctional nursing bed with integrated bed and chair: CN102038588A [P]. 2011-05–04.

8. Wang H, Xie L, Zhao X, et al. (2015) Mechatronics System Design and Experiment Research for a Novel Patient Transfer Apparatus. In: 3rd International Conference on Mechatronics, Robotics and Automation (ICMRA). Shang Hai. pp.1140-1143. DOI: 10.2991/icmra-15.2015.220.

9. Swedish Anjiu Company. (2017) Ceiling Lift Systems from Arjo Huntleigh Enable Residents/Patients to be transferred in a Safe, Comfortable and Dignified Way [EB/OL]. http://www.arjohuntleigh.com/products/patient-transfer-solutions.

10. Gan X, Wu X, Xu X, et al. (2012) Research and CAD design of a new multifunctional electric wheelchair [J]. Clinical Medical Engineering. DOI: 10.3969/j.issn.1674-4659.2012.07.1040.